Finite Element Modeling and Experimental Validation of Conventional and High Speed Shear Testing in Pb-Free Environment

Abhinav Ajmera[1], S. Manian Ramkumar[2] and Ti Lin Liu
Center for Electronics Manufacturing and Assembly
Rochester Institute of Technology
Rochester, NY 14623
Phone: 585-475-6081
Email: abhinav@mail.rit.edu[1], smrmet@rit.edu[2]

Abstract

With the extensive use of Pb-free solder in electronic assemblies, there is a growing concern about the reliability of the solder joint. The integrity of the intermetallics, formed during the reflow process, at the component–pad interface is one of the critical determinants of joint reliability. Studies indicate that the brittle fracture of intermetallic compound (IMC) at the component-pad interface makes Pb-free solder joints more vulnerable to failure. Pb-free alloys with a high content of Sn and high reflow temperatures; experience accelerated and thicker intermetallic formation at the interface [1]. The brittle intermetallics are susceptible to fracture during a major stress event, such as drop, over the entire life cycle of the joint [2]. This necessitates the investigation of possible approaches to predict and detect brittle fracture.

The tests that are available currently do little in this regard as they are incapable of consistently applying the force to demonstrate brittle fracture [3]. The low speed shear test has not been successful in generating bond failures, as the failure typically happens in the bulk of the solder joint. However, a high speed shear test may succeed in demonstrating the brittle fracture as they replicate high strain rate events [3]. The need to identify the capability of high speed shear, to reveal brittle fracture failures, was the driving force behind this study. Shearing of 0603 resistors mounted on a PCB with Pb-free solder was considered as the test process setup for modeling and experimentation. Finite Element Analysis (FEA) was employed to replicate the process of shearing the solder joint. A comparison was drawn between the FEA results and the results obtained through the actual lab testing.

The FEA results for the low speed shear test suggest that the failure would have a very high probability of occurrence in the bulk of the solder with the shear force ranging from 20-28 N. This range, predicted by FEA, was found to be 20% lower than the actual test results. Furthermore, FEA provides reasonable assurance about the capability of high speed shear to demonstrate brittle fracture at the intermetallic. Application of force in the range of 56-65 N would be required for this failure mode at the interface.

Moreover, the results establish Finite Element Analysis as a reasonable approach to illustrate the changing stress patterns that a component undergoes when subjected to shear. On the whole, the results of the analysis substantiate high speed (high force) shear being a promising test to predict and detect the brittle fracture failure of the Pb-free interconnects.

Introduction

The formation of intermetallic compounds (IMCs) during reflow soldering, involving a high percentage Sn-containing solder alloys, is inevitable. These IMCs are critical in achieving a strong metallurgical bond and their integrity determines the reliability of a joint. The very high percentage of Sn in Pb-free solder alloy (at least 95%) and the high reflow temperatures generate a thicker layer of intermetallic. These thick IMCs, with their very nature of being brittle, can prove to be detrimental to the reliability of the joint [4, 5]. Under high strain rate events like drop, thick intermetallics are more susceptible to brittle fracture. The present-day Pb-free electronic hand-held products are often subjected to major stress events during operation. It is critical to evaluate the strength of the joints for such applications where brittle fracture would be the primary failure mode [6].

The traditional reliability tests, such as the low speed shear, are not suitable for predicting joint reliability under drop loading. This is primarily because the applied test speeds are much lower than the impact velocities experienced by the assemblies under a high strain rate event [7]. In the low speed shear tests, the failure occurs in the bulk of the solder joint, as shown in Figure 1 (a), and not at the bond interface. Studies have proven that the strength of the solder alloy, regardless of Pb, increases with the increase in the strain rate [8]. Thus, failure in the bulk of the solder proves that the bond is as strong as or stronger than the applied force. This does not provide any inference on the actual bond strength between the solder and the component pad and the brittle fracture resistance [9]. The other solder joint reliability tests such as board level drop and shock, and the high speed shear tests provide better estimations of the brittle fracture resistance, by closely simulating the actual conditions of the high strain rate events. These tests produce more bond failures than their counterparts [9].

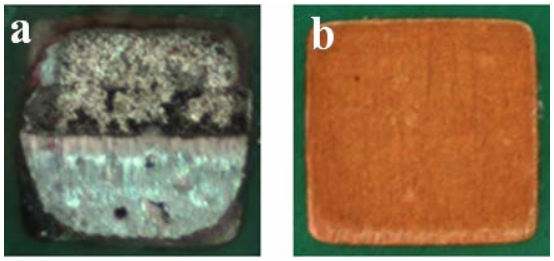

Low Speed Shear Test Result (Ductile Failure) **High Speed Shear Test Result (Brittle Failure)**

Figure 1. Ductile and Brittle Failure

Among all the three, the board level drop test is the oldest testing methodology and has been understood well. Whereas, the high speed shear testing has been introduced recently and is still evolving [9]. However, the board level drop test has major drawbacks. First, it is expensive both in terms of the time and resources, as each drop test consumes several packages and solder joints, and the data analysis is time-consuming. Second, in the absence of a real-time monitoring system, there is a possibility of not detecting a joint failure if the crack in the solder joint closes after impact [10]. With the inability of the drop test to meet the time frame to develop and market new electronic products, it has become imperative for the industry to consider other available alternatives. Recent studies comparing the board level drop test performance with high speed shear demonstrate significant correlation between the performances of the two tests [10]. This makes it critical for the industry to understand the high speed shear test.

High speed shear test, with speeds exceeding 1000 mm/sec replicate the high strain rate events like drop. Shearing at such high speeds transfers a much higher force from the solder matrix to the bond between the bulk of the solder and the component pad (intermetallics). This test is capable of qualifying the component-pad interconnection under impact testing [11]. A typical outcome of a brittle fracture induced by high speed shear is shown in Figure 1 (b).

However, this test is still new to the industry and the working principle needs to be addressed and well understood [9]. In order to have a better comprehension of the test, Finite Element Analysis (FEA) was employed in this study. This study intends to manifest the capability of high speed shear to demonstrate brittle fracture at the interface between the solder matrix and the component pad, with the help of FEA. If the industry is able to establish and understand the ability of high speed shear to detect brittle fracture, its utilization can then be further extended to compare performances of different surface finishes for Pb-free applications and different solder alloys.

For the analysis, a 3-D model of a Pb-free assembly comprising of 0603 resistors was considered. The assembly was subjected to Mechanical Event Simulation (MES) with Non-linear Material Models for simulating the shear process. Subsequently, to validate and better understand the FEA results, low speed and high speed shear tests were conducted to draw a comparison between the results obtained from FEA and experimentation.

Finite Element Analysis (FEA)

The accuracy and applicability of FEA results primarily depends on the dimensional accuracy of the model with adequate details regarding the material properties for the different sections of the assembly.

Modeling Methodology

The dimensions for the 0603 resistor were acquired from the design specification sheets for chip resistors. The measurements of the other sections of the solder joint were obtained from the cross-sections of the assemblies prepared for the experiment. The details of the solder joint are shown in Figure 2. Figure 2 (a) shows the right hand fillet of the joint and Figure 2 (b) shows the intermetallic layer.

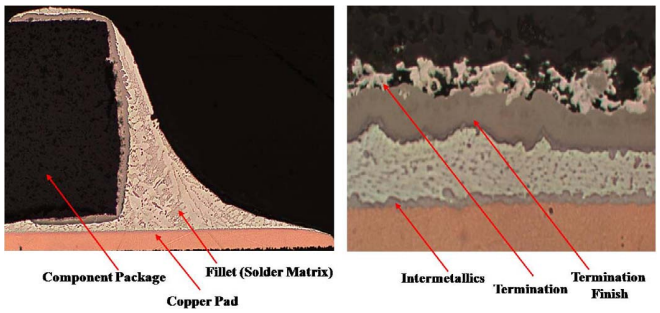

a) Right Hand Fillet **b) Intermetallic Layer**

Figure 2. Solder Joint

Based on the dimensions obtained, a 3-D model was created in SolidWorks and subsequently analyzed using ALGOR. An outline of the 3-D model and its dimensions are shown in Figure 3 and Figure 5 respectively. Due to the existing domain symmetry, only one half of the resistor was considered for the analysis. Symmetric boundary conditions would account for the other half of the resistor. The finite element mesh around the complete setup, illustrating different sections of the joint, is shown in Figure 4.

The model includes the most relevant sections for the mechanical behavior of the assembly. For ease of 3-D modeling and subsequent finite element meshing and analysis, the pad surface finish was ignored. To simplify the model, only one intermetallic (Cu_6Sn_5) was considered and the other possible intermetallics, Cu_3Sn and Ag_3Sn, were ignored. This is also in accordance with the findings of another research study, which suggests that the variation in thickness of the Cu_6Sn_5 intermetallic layer has a more severe influence than any other intermetallic [12].

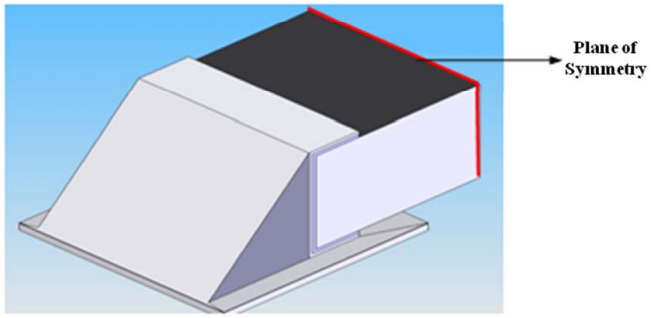

Figure 3. Outline of the 3-D Model of the Resistor

The wetting of the termination on the top was also not considered. The absence of the substrate in the assembly setup is accounted for, by defining zero degrees of freedom as boundary condition, for the bottom side of the copper layer.

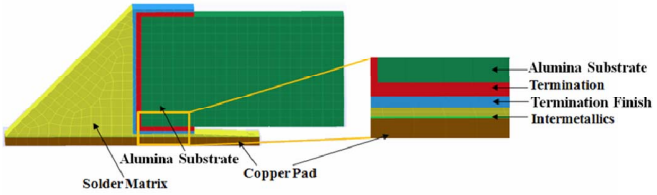

Figure 4. Finite Element Mesh of the Complete Setup

For the analysis of the results, three sites were considered for examining the stress distributions – the total setup, solder matrix and the intermetallic.

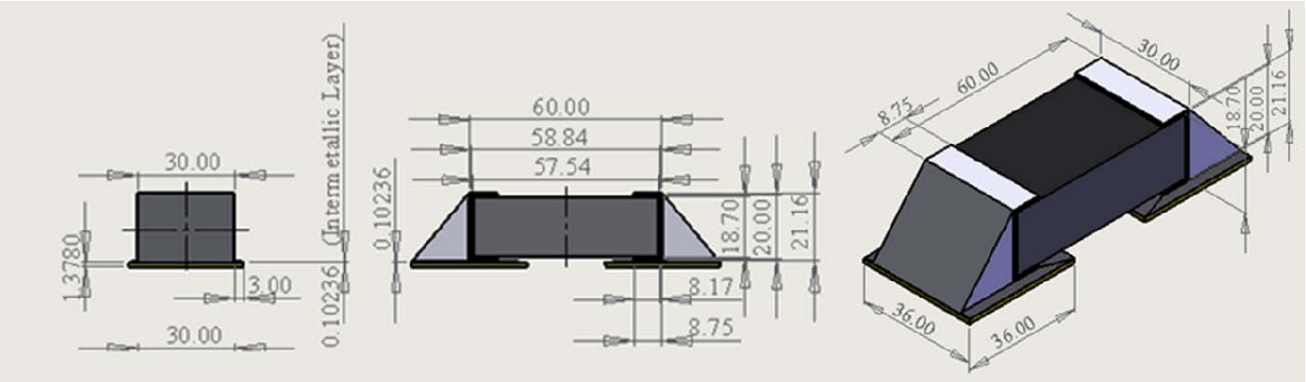

Figure 5. Dimensional Details of the Assembly

These sites were chosen in accordance with the different failure sites normally observed during low speed and high speed shear tests.

The analysis was carried out in two phases. These two phases differ in their approach to stress-strain relationship. Phase I deals with Static Stress with Linear Material Models (SSLMM), while Phase II deals with Mechanical Event Simulation with Nonlinear Material Models (MESNMM). Phase I analysis is restricted to the linear relationship of stress and strain, without entering into the deformation stage, while the Phase II analysis, goes past the linear relationship and enters into the region of plastic deformation.

SSLMM enables the study of stress, strain, displacement, shear and axial forces that result from static loading. This analysis parameter is often sufficient for situations in which loads are known and the time of peak stress is evident. It would provide an insight into the behavior of the assembly setup when its yield is approaching. However, it would not be able to demonstrate permanent deformation of any section. The need to demonstrate brittle fracture rules out the possibility of carrying out SSLMM. Therefore, consideration had to be given to some alternative analysis that could demonstrate stress and strain distributions beyond the linear relationship (MESNMM). For conducting MESNMM additional properties like the strain hardening modulus and yield stress were required. After a detailed literature review, these properties were obtained for all sections of the solder joint except the solder alloy (SAC305) and intermetallic (Cu_6Sn_5).

As the percentage of Copper (0.5%) is less in SAC305, it was substituted with Sn-3.5Ag; for which all the required properties were known. With the properties that were available for Cu_6Sn_5, it was possible to run only the SSLMM. After exploring the materials directory of the FEA software, properties of two materials – Niobium and Zirconium were found to match closely with the known Cu_6Sn_5 properties, with Zirconium being the closest. For Zirconium the strain hardening modulus and the yield stress were also available.

In order to verify the suitability of substituting Zirconium for Cu_6Sn_5, SSLMM was run twice; once with Cu_6Sn_5 and then with Zirconium as the substitute. The performances of the three possible failure sites were then compared. In Phase I, a comparison was also drawn between the performance of the assembly with termination finish (nickel end cap coated with tin) and without termination finish (nickel end cap only). This was to identify the effect of termination finish on the shear load bearing capacity of the component.

Phase I: Static Stress with Linear Material Models (SSLMM)

For carrying out SSLMM analysis in Phase I, a force of 30 N was applied along the length of the resistor, based upon prior experiments. The different sections of the assembly were regarded as isotropic, assuming that their material properties are identical in all directions. Furthermore, a solid mesh was considered with bricks and tetrahedral elements. The mesh size used for this analysis was 100%. The lateral length for which the force is applied was determined by considering the width of the shear tool used in the Dage 4000 low speed bond tester. The height for application of the force in the model was maintained the same as the shear height used in the experiment. The setup along with the boundary conditions is shown in Figure 6. The width of the tool is 1.27 mm and the shear height is 80 µm above the top surface of the board [13].

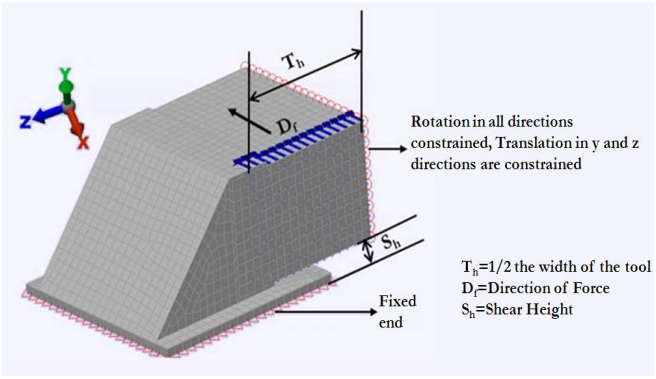

Figure 6. Setup for Finite Element Analysis

Table 1 provides a comparison between SSLMM analysis using Cu_6Sn_5 and zirconium. Table 2 provides a comparison between the SSLMM analysis with and without termination finish.

It can be observed from the comparison in Table 1 that except for a slight difference in the results for the IMC layer, there is not a considerable percentage difference between the other results. This provided the confidence to use Zirconium as a suitable substitute for Cu_6Sn_5.

The results in Table 2 strongly suggest that the assembly without termination finish experiences more stress and thus is more vulnerable to shear than the one with termination finish.

So, the presence of tin as the termination finish provides additional strength to withstand mechanical stresses.

Table 1. Comparison between Cu_6Sn_5 and Zirconium

Parameter (All Max. Values)	Zirconium	Cu_6Sn_5	% Difference
Total Stress	2.42e8 N/m^2	2.4e8 N/m^2	0.83%
Total Strain	0.0021	0.0021	0%
Total Displacement	7.64e-6 m	7.65e-6 m	-0.13%
Stress in Matrix	7.59e7 N/m^2	7.61e7 N/m^2	-0.26%
Strain in Matrix	0.0021	0.0021	0%
Displacement in Matrix	4.28e-6 m	4.29e-6 m	-0.23%
Stress in IMC	6.07e7 N/m^2	6.67e7 N/m^2	-8.99%
Strain in IMC	0.00086	0.0010	-14%
Displacement in IMC	8.66e-7 m	8.84e-7 m	-2.04%

Table 2. Comparison Between the Stress Values With and Without Termination Finish

Parameter (All Max. Values)	Without Termination Finish (a)	With Termination Finish (b)	% Difference [(a-b)/a]*100
Total Stress	2.42e8 N/m^2	1.2e8 N/m^2	50.4% More
Stress in Matrix	7.59e7 N/m^2	4.41e7 N/m^2	41.9% More
Stress in IMC	6.07e7 N/m^2	4.31e7 N/m^2	29% More

With all the properties required to run MESNMM available, Phase II was carried out. The material properties of the constituent sections are listed in Table 3.

Table 3. Material Properties

Serial Number	1	2	3	4	5	6
Part	Component	Termination	Termination Finish	Solder Paste Matrix	Intermetallic Layer	Pads
Material	Alumina (Al_2O_3)	Nickel (Ni)	Tin (Sn)	Tin-Silver-Copper (Sn-Ag-Cu)	Cu_6Sn_5	Copper (Cu)
Material Considered	Alumina (Al_2O_3)	Ni Typical	Tin	Tin-Silver	Zirconium	Copper Cold Drawn
Density Kg/m^3	3985	8880	5765	7440	6530	8960
Modulus of Elasticity (Pa)	1.67E+11	2.07E+11	4.14E+10	5.08E+10	9.45E+10	1.10E+11
Poisson's Ratio	0.22	0.31	0.33	0.4	0.34	0.364
Ultimate Tensile Strength (Pa)	4.21E+08	3.17E+08	2.22E+08	2.63E+07	3.30E+08	3.44E+08
Yield Strength (Pa)	2.88E+08	5.90E+07	-	2.50E+07	2.30E+08	3.33E+08
Shear Modulus (Pa)	6.84E+10	7.9E+10	1.56E+10	1.814E+10	3.53E+10	4.03E+10
Ductile Elongation (%)	0.32	0.3	-	0.48	0.32	0.14
Strain Hardening Modulus (Pa)	4.16E+08	8.60E+08	-	2.71E+06	3.13E+08	7.57E+07
Source	NASA	Matweb	Matweb	NIST	Matweb	Matweb

Phase II: Mechanical Event Simulation with Nonlinear Material Models (MESNMM)

This analysis combines kinematic, rigid and flexible-body dynamics and nonlinear stress analysis capabilities. As a result, MESNMM can simultaneously analyze mechanical events involving large deformations, nonlinear material properties; kinematic motion and forces caused by that motion and then predict the resulting stresses. This analysis has the ability to demonstrate permanent deformation, which was a limitation of SSLMM. For carrying out MESNMM, a force of 100 N was applied along the length of the resistor, in increments of 1 N. The boundary conditions and the model being considered remain the same as considered in the SSLMM analysis. The mesh size for this analysis was 100% with the dimensional and force tolerances as 0.001. The load curve, which is a multiplier of the load over time, is shown in Figure 7. This curve reveals that there would be a uniform increase in the load with time. The material model is assumed to be von Mises with Isotropic Hardening.

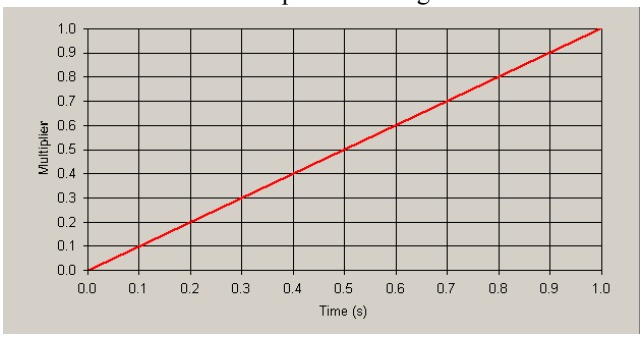

Figure 7. Load Curve

Stress Analysis – MESNMM

In this analysis, the stress experienced by the total setup would be much higher than that experienced during the SSLMM analysis. This is primarily because of the application of a greater magnitude of force. The stresses observed for the total setup, the solder matrix and the intermetallic layer after the application of 100 N are shown in Figure 8.

It can be observed that the maximum stress is experienced by the termination finish in the total setup. The stress is concentrated along the surface where the termination finish makes contact with the solder matrix.

However, under the influence of this high magnitude of force, the stress experienced by the intermetallic is greater than the stress experienced by the solder matrix. The observed maximum stress in the solder matrix (2.91e8 N/m^2) is much greater than the yield stress of the matrix (2.5e7 N/m^2). This indicates that the solder matrix would be sheared under this magnitude of force. Additionally, the observed maximum stress in the intermetallic layer (9.43e8 N/m^2) is also greater than its yield stress (2.3e8 N/m^2). This suggests that at this force the intermetallic layer would also be sheared. This also gives a hint about the brittle nature of intermetallics that makes the solder joint weak.

Even though the observed maximum stress for both the solder matrix and the intermetallic are higher than their respective yield stress, the chances of shear are higher at the intermetallics. This can be attributed to the fact that the maximum stress is transferred to this interface. To better understand the mechanism behind the stress distribution, at different interfaces in the assembly and at different applied shear force, the maximum stress experienced by different interfaces were recorded and a graph was plotted, which is shown in Figure 9.

From the graph it can be observed that the region 'A' corresponds to the period wherein there is a high probability of failure in the solder matrix with intermetallic fracture highly unlikely. Moreover, region 'A' relates to the ductile failure in the solder matrix during a low speed shear test.

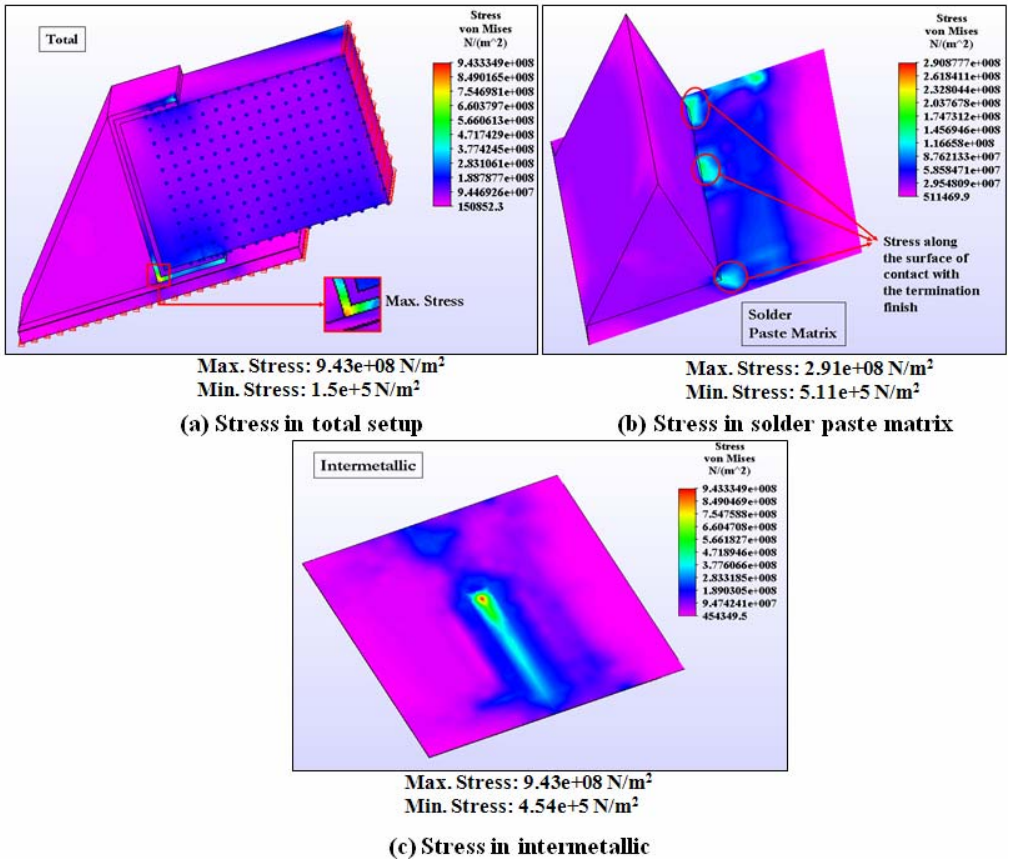

Figure 8. Stress Distribution in the Total Setup and Different Interfaces

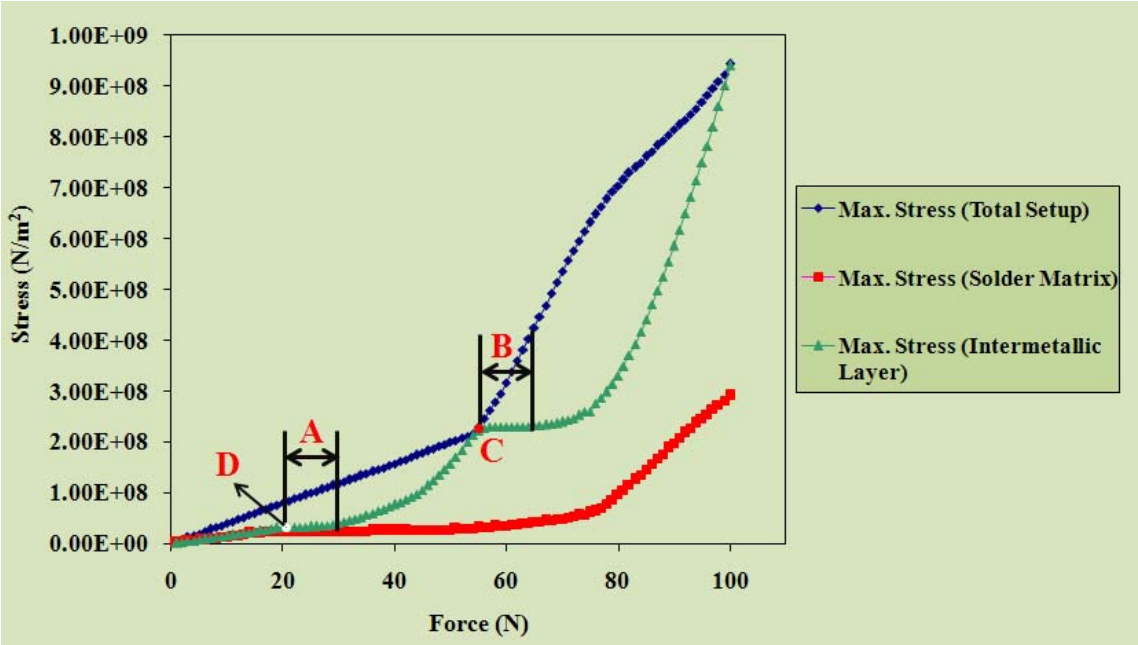

Figure 9. Maximum Stresses in the Total Setup and Different Interfaces

The ductile failure is primarily because the applied stress has exceeded the yield stress of the solder matrix, but has not reached the yield stress of the intermetallic. The shear stress experienced by solder matrix until point "D", is either higher than or equal to the shear stresses experienced by the intermetallic. Therefore, the chances of failure to occur in the solder matrix are higher. The graph also suggests that there is a very high possibility of failure to occur in the bulk of the solder if the applied shear force is in the rage of 20-28 N.

Region 'B' corresponds to the period where there is a high probability of brittle fracture at the intermetallic. This is a region where a very high magnitude of force is applied and

transferred to the intermetallic, which is possible in a high strain rate event. Furthermore, this FEA finding aligns with the theory that at a high speed, a much higher force is transferred from the solder matrix to the bond between the bulk of the solder and the component pad interconnect (intermetallics) causing the brittle fracture [11]. The graph also suggests that the applied shear force at which the brittle fracture will possibly occur, ranges from 56-65 N. It can be observed from the graph that at point "C", the maximum stress in the total setup is experienced by the intermetallic. This is the point from which the failure is likely to be initiated.

For an enhanced understanding on the way high shear forces and stresses are transferred to the solder matrix and intermetallic, the Stress Concentration Factor (SCF) was calculated for the assembly. SCF, in the area of a stress raiser, is a ratio of the maximum stress to the corresponding nominal stress. It is a theoretical indication of the effect of stress concentrators on mechanical behavior. For the calculation of the SCF, nominal stress was required to be calculated; as shown below:

$$\text{Nominal Stress} = \sigma = \frac{P}{A_s}$$

where, P = Load Applied = 100N

A_s = Area under shear loading

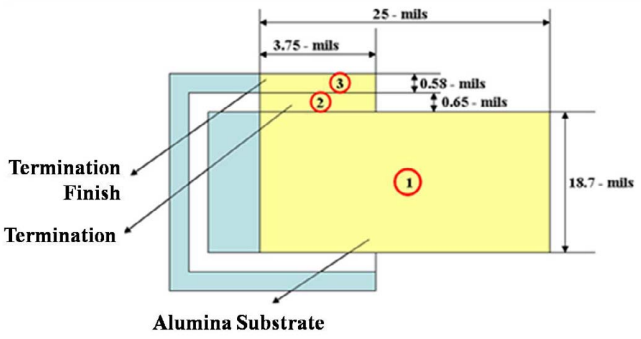

Figure 10. Area under Shear Loading

The shear area includes major part of the resistor and some portions of termination and termination finish. If the entire resistor is considered, as shown in Figure 10, only certain sections (1,2 and 3) are under the shear loading. This is in agreement with the shear height employed for carrying out the low speed shear tests.

Based on Figure 10, the area under shear loading includes:

$$\Sigma(\text{Area of Alumina Substrate, Area of Termination, Area of Termination finish}) = (25*18.7) + (3.75*0.65) + (3.75*0.58) = 472.11 \text{ mils}^2 = 3.05\text{e-}7 \text{ m}^2$$

$$\therefore \sigma = \frac{100}{3.05e-7} = \mathbf{3.28e+8\ N/m^2}$$

For the section considered in the FEA study (point A, B, C and D), the maximum stress is obtained from FEA (Figure 11). By calculating the SCF for each point, which ranges between 0.04-2.8, it's evident that the stress concentration is predominant at point C, point A and point D. It can be further concluded that these points, which are on the termination finish, are critical for the strength of the joint and measures should be taken to reduce stress concentration at these points.

For point A, SCF = 4.24e+08/ 3.28e+08 = **1.3**
For point B, SCF = 1.26e+07/ 3.28e+08 = 0.04
For point C, SCF = 9.06e+08/ 3.28e+08 = **2.8**
For point D, SCF = 3.86e+08/ 3.28E+08 = 1.18

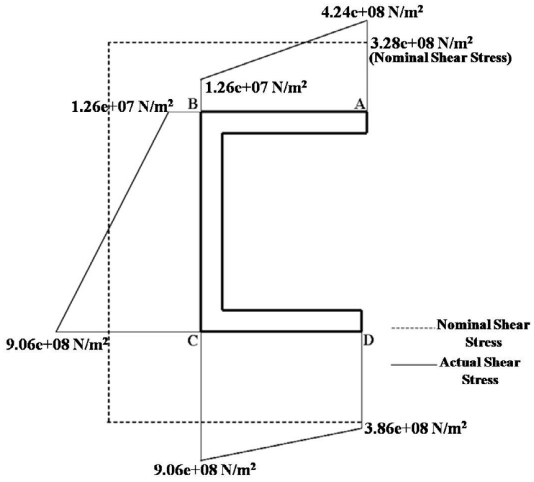

Figure 11. Stress Distribution

Figure 12 shows the regions for high stress concentration, obtained by FEA.

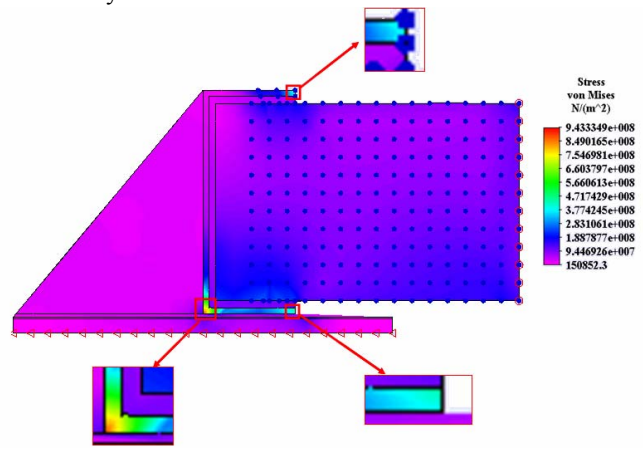

Figure 12. Regions of High Stress Concentration Factor

Issues with the termination finish are more likely to be observed during a low strain rate event as the chances of failure of the intermetallic are bound to happen only at high strain rates. This correlates with the low speed shear test. From this SCF calculation it can be understood how the termination finish transfers stresses to the solder matrix and intermetallic and why the shear in the low speed shear test occurs along the surface of the termination finish.

Experimental Validation

To validate the claims made by the FEA study, tests were executed to understand the processes of low speed shear and high speed shear.

Test Vehicle

The layout of the test vehicle used for the study is shown in Figure 13. Twelve 0603 resistors were assembled on each test vehicle with OSP finish. The paste used for the assembly was SAC305.

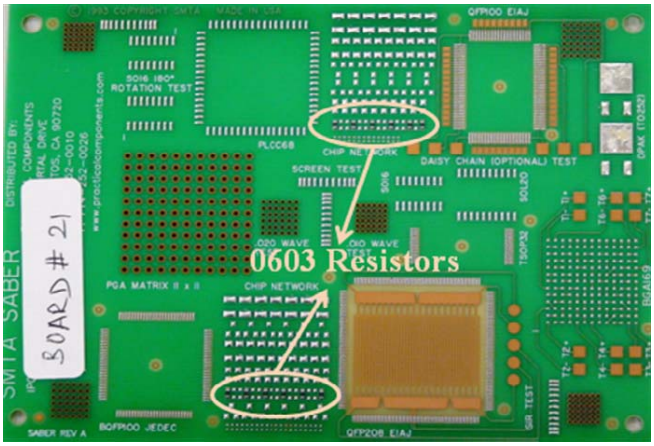

Figure 13. Test Vehicle

Direction of Shear

Most of the literature on shear tests pertained to BGA ball shear. The limited literature regarding resistor shear suggests that the direction of shear should be perpendicular to the length of the resistor, as shown in Figure 14 (a) – longer side shear. This implies that the tool should apply the force to both the resistor joints simultaneously, subjecting the joints to shear loading. However, no study has attempted to shear resistors from the shorter side, i.e. the tool travelling in line with the joints, as shown in Figure 14 (b) – shorter side shear. This implies that the tool initially comes in contact with one joint, shears it and pushes it further to shear the other joint. In this study, the shear test was executed from both the sides.

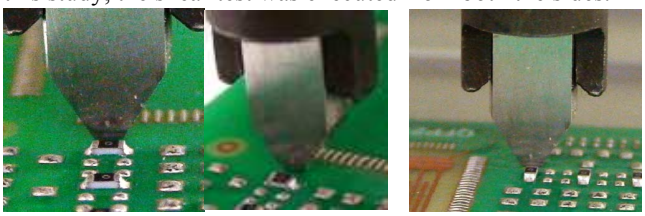

(a) Longer Side Shear **(b) Shorter Side Shear**

Figure 14. Directions of Shear

Experimental Setup

Shear Test

The testing was carried out in two phases. Phase I was low speed shear tests from the longer and shorter side and Phase II was high speed shear tests from the shorter side only. The high speed shear from the shorter side only was because of the unavailability of the appropriate tool to conduct high speed shear from the longer side. By conducting the low speed shear test from both the sides, this study attempted to find some correlation between the shear force readings. Further details of the two experimental phases are given below:

Phase I: Low Speed Shear Tests

A Dage-Series 4000 bond tester was used for conducting the low speed shear tests and collecting the shear strength data of the joints. In shear testing, shear rate (speed) and shear tool height are important parameters. In an attempt to establish a correlation between the shear speeds and shear force, speeds were varied from 100-700 µm/s and corresponding shear forces were recorded. A minimum of 10 observations for each speed variation were taken. A summary of various sample and test parameters is listed in table 4.

Table 4. Parameters for Low Speed Shear Tests

Parameter	Description
Test Method	Low speed shear test
Load Cartridge	100 kg
Loading Rates	100, 200, 200, 400, 500, 600, 700 µm/s
Shear Height	80 µm [13]
Fall Back	90%
Test Load	4.9 N
Shear Directions	Longer side, Shorter side
Components	0603 resistors
Solder Composition	Sn3.0Ag0.5Cu
Pad Finish	OSP
Sample Status	As soldered

Results and Discussions – Low Speed Shear Test

Shear testing and cross-sectional analysis were performed to determine the shear strength of the joints and the failure mode. For the purpose of comparing the FEA results with the actual test results, shear rate of 300 µm/s was chosen. This speed is based on previous studies [14]. In accordance with the direction in which the forces were applied during FEA, experimental shear test data for the longer side were considered for the comparison.

Comparison between FEA and Test Data

The probability plot of the shear data obtained from longer side low speed shear at 300 µm/s is shown in Figure 15. It can be observed that the data indicates good normality. The plotted data follow the fitted distribution line closely. With a p value>0.05 (0.67), it can be said that a normal distribution with mean of 27.65 N and standard deviation of 2.549 fits the recorded data fairly well.

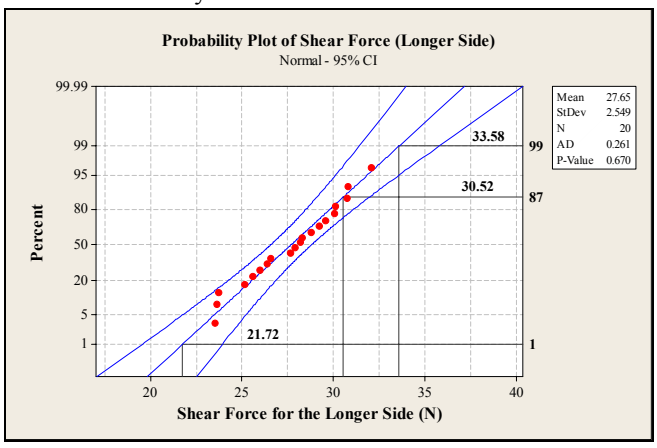

Figure 15. Probability Plot of Shear Force

Based on the probability plot, with a 95% confidence level, it can be concluded that the shear force values for the longer side low speed shear ranges between 21.72-33.58 N. The FEA results predicted a range of 20-28 N, with a difference of approximately 20%. This difference can be attributed to the design assumptions considered during FEA modeling. This confirms the ability of FEA to simulate low

speed shear tests and also establishes Zirconium as a suitable substitute for Cu_6Sn_5.

Another important finding of the FEA study was with regards to the failure mode in low speed shear. FEA suggested that for a 0603 resistor, the failure will occur in the solder matrix. The cross-sectional analysis of the sheared joint confirms that the failure, ductile in nature, occurred in the bulk, as shown in Figure 16.

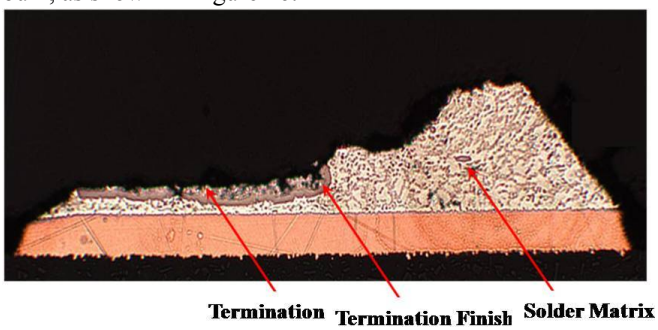

Figure 16. Cross-sectional Analysis of a Sheared Joint

The cross-sectional image in Figure 16 also shows some traces of termination finish still left over. This suggests that the failure was initiated through the termination finish, which correlates to the SCF calculations. This calculation also indicated that termination finish is very critical for the strength of the joint.

Speed and Directional Variations

The shear rate was varied from 100-700 µm/s, in steps of 100 µm/s. Resistors were sheared at these variations from both the longer and shorter sides. The probability plots for both the longer and the shorter side shears at the seven different speed variations are shown in Figure 17.

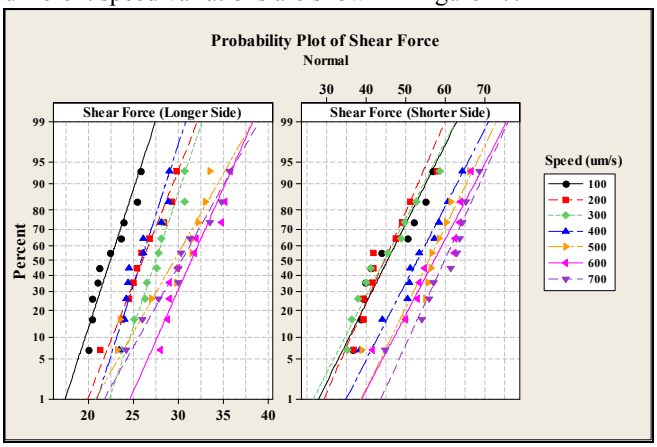

Figure 17. Probability Plot for Shear Force for the Longer Side and the Shorter Side

With the p-value>0.05 for all the plots, it can be concluded that the data collected for different speed and shear direction combinations are normal.

A plot showing the shear speed and mean shear force, for both the longer and the shorter side shear, provides an insight into the correlation between the shear from the two directions. It is evident from the plot, shown in Figure 18, that the shear force is always much higher when sheared from the shorter side. This can be attributed to the resistance offered by the other joint that is not in contact with the shear tool.

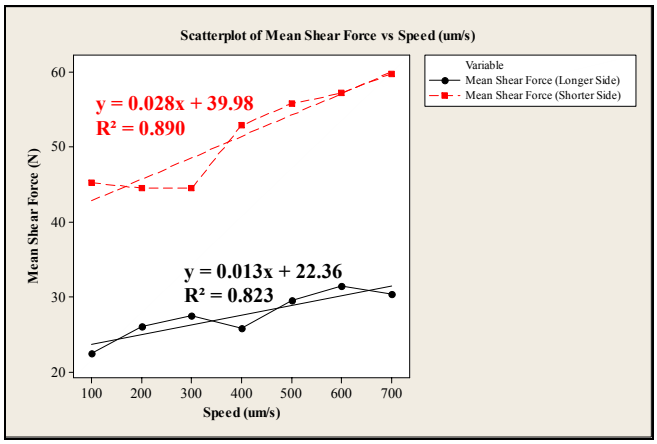

Figure 18. Scatterplot of Mean Shear Force (Longer Side), Mean Shear Force (Shorter Side) vs. Speed

It is because of this resistance that the shearing of the resistor leaves a very flat surface of solder matrix on the joint that is in contact with the shear tool, whereas a fillet on the other joint. The cross-sectional images of sheared joints of the resistor from the shorter side are shown in Figure 19.

With R^2 values greater than 80% in both the regressions, it is evident from Figure 18 that the shear forces for both the longer and the shorter side shear demonstrates an increasing linear trend with the increase in shear speed. This also shows that the resistance to shear of the solder matrix increases with the increase in the shear rate. This is the primary reason for the failure to occur in the solder matrix in low speed shear, which corresponds to a low-strain-rate event.

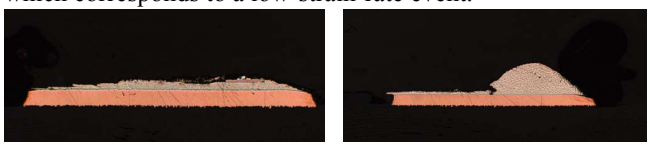

(a) Sheared In-contact Joint (b) Sheared Off-contact Joint

Figure 19. Sheared Joints from a Shorter Side Low Speed Shear

This relationship between the shear force and shear rate that exists during the low speed shear may not be applicable in high speed shear. At high speeds, with speeds in the range of 1-4 m/s, the solder strength cannot be evaluated as the failure site changes due to the change in the failure mode. During such a simulation of high strain rate event, the intermetallic strength turns out to be lesser than the solder strength. This is precisely the reason why the chances of occurrence of brittle fracture at the intermetallic are expected to increase in high speed shear. Theoretically, this can happen only when a higher magnitude of force is applied in a short period of time.

Phase II: High Speed Shear Tests

With the assistance provided by Dage Precision Industries, high speed shear tests were carried out using the Dage-Series-4000HS bond tester. However, as the industry utilizes bond testers primarily for ball shear, adequate shear tools were not available to execute the resistor shear from the longer side. The test and sample parameters of the high speed shear test are listed in Table 5.

Table 5. Parameters for High Speed Shear Tests

Parameter	Description
Test Method	High speed shear test
Load Cartridge	5 kg
Loading Rates	2.2 m/s
Shear Height	70µm
Shear Directions	Shorter side
Components	0603 resistors
Solder Composition	Sn3.0Ag0.5Cu
Pad Finish	OSP
Sample Status	As soldered

Results and Discussion – High Speed Shear Test

The high-speed shear tests were carried out at a shear speed of 2.2 m/s. To have a better understanding of how the high speed shear differs from the low speed shear, a comparison had been drawn between the shear force values of the two shear test methodologies from the shorter side. The shear force values for 300 µm/s were considered for low speed shear. A graph for the two data sets is shown in Figure 20.

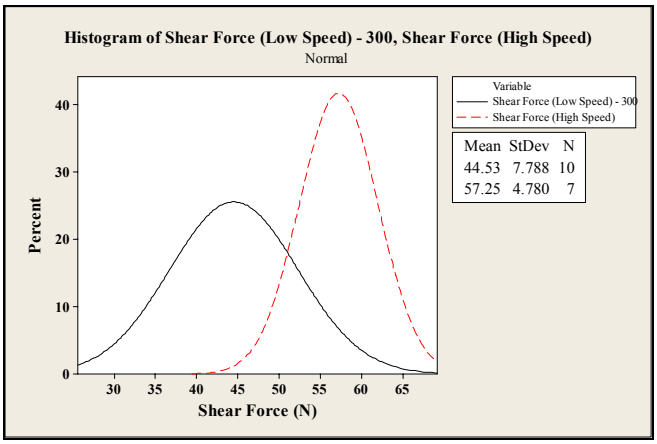

Figure 20. Comparison of Low Speed and High Speed Shear

It is evident from the graph that the mean shear force for the high speed shear tests is much higher than the mean shear force for the low speed shear test. This is indicated by the means (57.25 and 44.53 N respectively) shown in the table within the graph, as well as the relative position of the peaks for the fitted normal distribution. The standard deviation for low speed (7.780 N) is greater than the high speed (4.780 N), indicating that the high speed has better consistency in applying high forces.

Even though graphically there seems to be a difference in the shear forces, a 2-sample t-test was performed to determine if the difference observed was statistically significant.

Two-Sample T-Test and CI: Shear Force (Low Speed), Shear Force (High Speed)

Null Hypothesis: H0 = µ(Low Speed)-µ(High Speed) = 0

Alternative Hypothesis: H1= µ(Low Speed)<µ(High Speed)

With p-value<0.05, it can be inferred that the difference between the mean shear forces for the low speed and high speed shear tests is statistically significant.

Two-sample T for Shear Force (Low Speed) vs Shear Force (High Speed)

	N	Mean	StDev	SE Mean
Shear Force (Low Speed)	10	44.53	7.79	2.5
Shear Force (High Speed)	7	57.25	4.78	1.8

Difference = mu (Shear Force (Low Speed)) - mu (Shear Force (High Speed))
Estimate for difference: -12.73
95% upper bound for difference: -7.35
T-Test of difference = 0 (vs <): T-Value = -4.17 P-Value = 0.000 DF = 14

It can be concluded from the histogram and the 2-sample t-test that the shear force is higher in case of high speed shear. This further confirms the inference drawn earlier with regard to the relationship between the solder strength and the shear rate. The increase in the shear force also suggests an increase in the force applied to the joint. This shows that with the increase in shear rate the solder strength of the matrix is increasing with a possible decrease in the strength of the intermetallic. Table 6 summarizes the existing relationships between the solder strength, the intermetallic strength, the failure mode and the shear rate.

Table 6. Failure Modes and Shear Rate

Solder Strength	Intermetallic Strength	Failure Mode	Failure Site	Shear Rate
Low	High	Ductile	Solder Matrix	Low
High	Low	Brittle	Intermetallic	High

However, it was also observed that the sheared joints obtained from the high-speed shear from the shorter side do not demonstrate brittle fracture. With the mode of failure still ductile and the failure site still the solder matrix, it can be further concluded that the shear from the shorter side, irrespective of the speed, has a very low possibility of inducing brittle fracture in the intermetallic.

Conclusions

The following are the major conclusions that can be derived from this work:

1. FEA is a reasonable source to analyze and understand the principle and mechanism of both high speed and low-speed shear tests.
2. Zirconium proves to be a reasonable substitute for Cu_6Sn_5.
3. Termination finish improves the mechanical strength of the joints significantly
4. The failure of the joint initiates through the termination finish of the joints
5. Brittle fracture at the intermetallic cannot occur or even be initiated at low shear rates. At low shear rates, the failure site will primarily be the solder matrix.
6. Shorter side shear is less likely to shear at the intermetallic even at high shear rates.
7. The strength of the solder is directly proportional to the shear rate (speed). Higher the shear rate, higher is the solder strength exhibited by the solder matrix.
8. A brittle fracture can happen only when the solder strength is greater than the intermetallic strength.

9. In high speed shear test, a greater magnitude of force is applied in a short period of time, instigating the brittle fracture at the intermetallic.
10. The shear force required to cause joint failure during the shorter end shear will always be greater than the shear force during the longer end shear
11. The magnitude of force applied by the high speed shear would be greater than that applied by the low speed shear.
12. High speed shear certainly simulates the high strain rate events like drop.

Acknowledgment

The authors would like to acknowledge the support of Ms. Cynthia Andersen and Dr. Evstatin Krastev of Dage Precision Industries in carrying out the high speed shear tests. The authors are also grateful to Mr. David Fister, Senior Staff Engineer in Materials Engineering Laboratory at RIT for his support in material analysis. A thank is due to Jeff Lonneville, lab technician in the Center for Electronics Manufacturing and Assembly for his support in setting up the assembly and analysis equipment. Thanks are also extended to Mr. Sreekanth Penmatsa, Ms. Aarthi Baskaran and Mr. Sathish Kumar Sakthivelan, Graduate Research Associates, for their assistance in cross-sectioning and image analysis.

References

1. Lee, K. Y.; Li, M.; Olsen, R. D.; Chen, W. T.; Tan, B. T. C. and Mhaisalkar, S., "Microstructure, Joint Strength and Failure Mechanisms of Sn-Pb versus Pb-Free Solders in BGA Packages", *IEEE Transactions on Electronics Packaging*, Vol. 25, No. 5 (2002), pp 185-192
2. Vianco, P. T.; Erickson, K. L. and Hopkins, P. L., "Solid State Intermetallic Compound Growth Between Copper and High Temperature, Tin-Rich Solders", Journal of Electronic Materials, Vol. 23, No. 8, (1994), pp 721
3. Newman, K., "BGA Brittle Fracture – Alternative Solder Joint Integrity Test Methods", Electronic Components and Technology Conference, (2005), pp. 1194-1201
4. Blair, H. D.; Pan, Tsung-Yu; Nicholson, John M.; Cooper, Ronald P.; Oh, Sung-Won and Farah, Ahmad R., "Manufacturing Concerns of the Electronic Industry Regarding Intermetallic Compound Formation During the Soldering Stage", IEEE/CPMT International Electronics Manufacturing Technology Symposium, (1999), pp. 282-292
5. Fields, R. J. and Low, S.R., "Physical and Mechanical Properties of Intermetallic Compounds Commonly Found In Solder Joints", http://www.metallurgy.nist.gov/mechanical_properties/solder_paper.html
6. Lai, Yi-Shao; Yeh, Chang-Lin; chang, Hsiao-Chuan and Kao, Chin-Li, "Ball Impact Responses and Failure Analysis of Wafer-level Chip-scale Packages", Electronics Packaging Technology Conference, (2006), pp. 179-184
7. Song, F.; Lee, S. W. R.; Newman, K.; Sykes, B. and Clark, S., "Brittle Failure Mechanism of SnAgCu and SnPb Solder Balls during High Speed Ball Shear and Cold Ball Pull Tests", Electronic Components and Technology Conference, (2007), pp. 364-372
8. Hasegawa, K.; Takahashi, A.; Noudou, T. and Nakajima, S., "Electroless Ni-P/Pd/Au Plating for Semiconductor Package Substrate", Journal of SMT, Vol. 14, No. 1 (2001), pp. 17-22
9. Borgesen, P. and Sykes, B., "Predicting Brittle Fracture Failures", SMT Magazine, (2005), pp. 16-17
10. Song, F.; Lee, S. W. R.; Newman, K.; Sykes, B. and Clark, S., "High speed Solder Ball Shear and Pull Tests vs. Board Level Mechanical Drop Tests: Correlation of Failure Mode and Loading Speed", Electronic Components and Technology Conference, (2007), pp. 1504-1513
11. Laura, P., "Lead-Free Brings Out Problem of Brittle Fracture", Semiconductor International, (2005), 28(11), pp. 38
12. Madeni, J.; Liu, S. and Siewert, T., "Intermetallics Formation and Growth at the Interface of Tin-Based Solder Alloys and Copper Substrates", 2nd International Brazing and Soldering Conference, San Diego, CA, February. 2003
13. Sampathkumar, M.; Rajesnayagham, S.; Ramkumar, S. M. and Anson, S. J., "Investigation of the Performance of SAC and SAC-Bi Lead-Free Sodler Alloys With OSP and Immersion Silver PCB Finishes", SMTA International, (2005), pp. 568-575
14. Bukhari, S.; Santos, D. L.; Lehman, L. P. and Cotts, E., "Evaluation of the effects of Processing Conditions on Shear Strength and Microstructure in Pb-free Surface Mount Assembly", Journal of SMT, Vol. 17, No. 2 (2004), pp. 42-47